*ENGINEERING TRANSACTIONS* • *Engng. Trans.* • **43**, 1–2, 259–277, 1995
Polish Academy of Sciences • Institute of Fundamental Technological Research

# DYNAMIC CALCULATION OF THE YOUTH BRIDGE OVER THE DANUBE RIVER IN BRATISLAVA (*)

J. MELCER (ŽILINA)

The new bridge was built over the Danube river in Bratislava. Prior to opening of the bridge, its dynamic calculations were done according to the Czecho-Slovak Standard. The natural frequencies and modes of free vibration were calculated. The calculations were done in several variants using the finite element method. As a control method, the so-called Kolousek's slope deflection method was used. In the next step, the values of the dynamic coefficients were numerically simulated. The dynamic coefficients were determined from the bridge response produced by simultaneous runs of two vehicles arranged in one row, as they crossed the bridge. All numerically obtained results were tested by experimental measurements of the structure.

## 1. INTRODUCTION

According to the Czecho-Slovak Standard CSN 73 6209, the dynamic loading test is required prior to opening the bridges with the spans longer than 50.0 m to the traffic. During the test, the following characteristics are determined and analyzed:

a) The dynamic effectiveness of a loading vehicle,

$$\eta = \frac{S_{\mathrm{dyn}}}{S}, \tag{1.1}$$

where $S_{\mathrm{dyn}}$ is the calculated value of static deflection of the considered bridge span, caused by the test load for the dynamic test, while $S$ is the calculated value of deflection of the span under the design live load.

b) The measured dynamic coefficient $\delta$ expressed by the formula

$$\delta = \frac{S_{\max}}{S_m}. \tag{1.2}$$

c) Natural frequency of vibration of the unloaded bridge $f$.

(*) Paper presented at 30th Polish Solid Mechanics Conference, Zakopane, September 5–9, 1994.

d) Frequency of vibration of the loaded bridge $f$.

e) The logarithmic damping decrement $\vartheta$ according to the formula

$$\vartheta = \frac{1}{i} \ln \frac{S_{\text{fund}}}{S_1}. \tag{1.3}$$

All the symbols used are explained in Fig. 1.

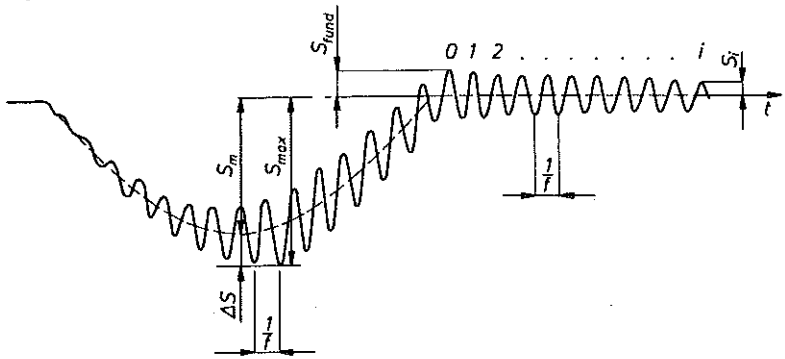


FIG. 1. Histogram of bridge vibration.

According the Standard, the basic criterion for dynamic evaluation of the bridge is expressed in the form

$$(\delta - 1)\eta \leq (\delta^* - 1), \tag{1.4}$$

where $\delta$ is the measured dynamic coefficient, and $\delta^*$ is the design dynamic coefficient.

The condition (1.4) should be fulfilled at least for 90% of all vehicles travelling over the bridge during the dynamic tests. The rest of tests should be in accordance with the relation

$$(\delta - 1)\eta \leq 1.1(\delta^* - 1), \tag{1.5}$$

some of the symbols used are explained in Fig. 1.

## 2. CHARACTERISTICS OF THE BRIDGE INVESTIGATED

The bridge investigated is the fourth in the series of bridges constructed across the Danube river in Bratislava. This bridge is located along the future express highway from Bratislava to Vienna. The bridge is proposed as two separate structures, one structure for one direction (strip) of the highway. The dynamic calculation presented below concerns the so-called "right-hand bridge".

In the final structural solution, the bridge is proposed to be a seven-span continuous beam with one frame column at the pier number 3 (cf. Fig. 2). The spans lengths are 83.0 m + 174.0 m + 172.0 m + 86.74 m + 3 × 83.0 m. No intermediate expansion joints are proposed in the superstructure.

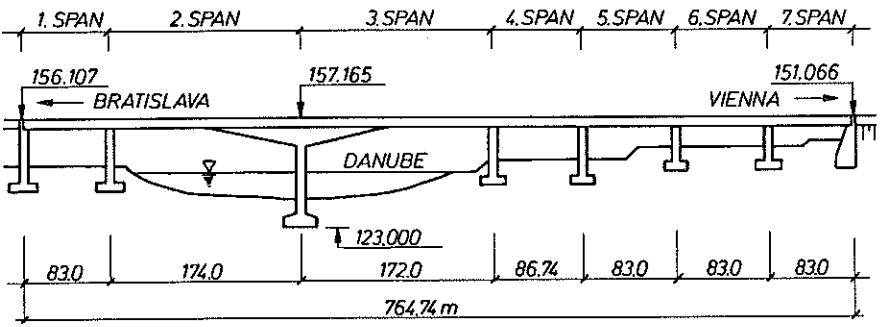


FIG. 2. Elevation of the bridge.

The cross-section of the main part of the bridge is a box shown in Fig. 3. The thickness of the webs and bottom slab is variable along the bridge as it is also shown in the figure.

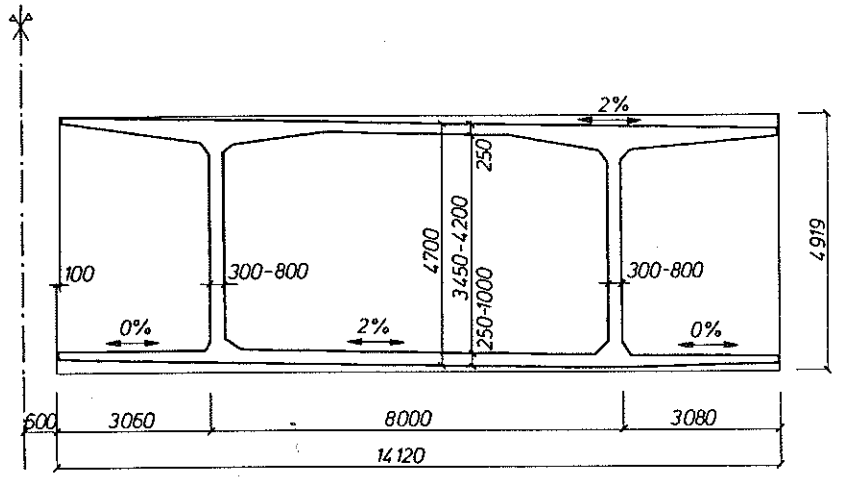


FIG. 3. Cross-section of the bridge superstructure.

The bridge is constructed as a monolithic structure made of prestressed concrete with the quality of B 500. Prestressing forces are proposed to be introduced by means of the tendons created from 12 plaited ropes of type $\phi LP$ 15.5/1 800. The prestressing is concentrated only in the top and bottom slabs of the box cross-section of the bridge superstructure. Further, the so-called free cables, which cover the effects of the moving loads and creep of

the concrete, are proposed. Moreover, the conventional reinforcement with the reinforcement ratio of 2% is placed in the bottom slab along the whole bridge to reduce the influence of creep, to improve the stiffeness and the loading capacity of the superstructure.

The bridge piers are monolithic and made of concrete B 400. The pottery type bridge bearings are applied for the structure.

The bridge is designed for the load class "A" according to Standard CSN 73 6203, Version "a" [3].

## 3. Natural frequencies and natural modes

### *3.1. Computing models*

Computation analysis was performed in the two following steps:

1. The plane dynamic behaviour of the structure was considered.
2. The spatial dynamic behaviour of the structure was considered.

In the first step, two models of the structure shown in Fig. 4 were chosen and analysed.

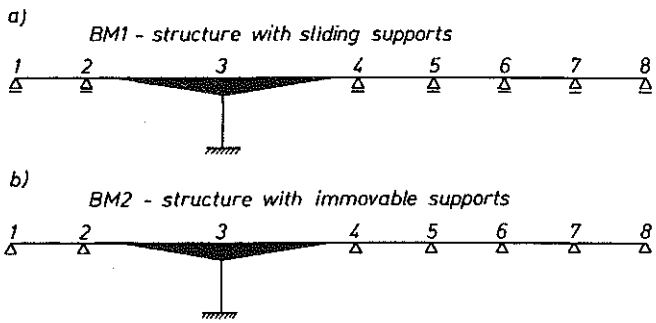


Fig. 4. Plane computing models of the bridge.

In the second step, two models shown in Fig. 5 were chosen and analysed. Transverse effect of the columns in the horizontal direction was substituted by the effect of the elastic springs with equivalent rigidities.

To determine the rigidity of the structure as true as possible, several combinations were taken into consideration.

First, two moments of inertia were considered:

I – moment of "net" concrete cross-section.

II – moment of equivalent concrete cross-section.

Second, three other cases were considered, namely:

A – area of the cross-section of superstructure without any bridge equipment elements;

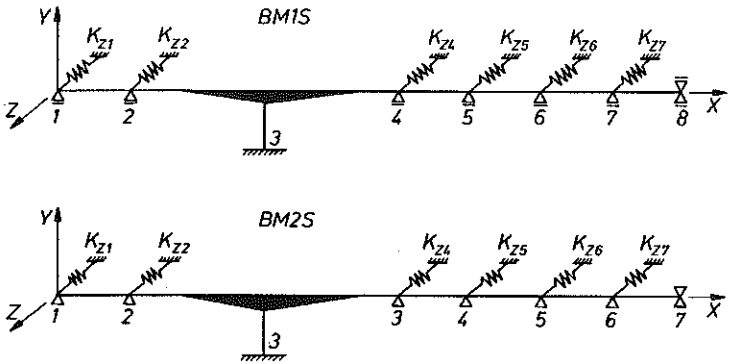


FIG. 5. Space computing models of the bridge.

B – area of the cross-section of the superstructure including the areas of drainage launders and concrete railings at the footways;

C – area of the cross-section of superstructure including the areas of drainage launders and concrete railings at the footways as well as pavement on the roadway and footways.

Therefore, the following combinations were considered and denoted respectively by IA, IB, IC or IIA, IIB, IIC.

The mass of a fully equipped bridge was assumed for dynamic calculations.

### *3.2. Results of computation*

To assure a control of the results of computation, the following three methods concerning the plane models analysis were used:

1. Rayleigh's energy method (REM),
2. Finite element method (FEM),
3. Kolousek's slope deflection method (KSDM).

Approximate calculation of the first natural frequency of the lateral vibration of the bridge for the model BM2 (cf. Fig. 4) was done by the Rayleigh's energy method and led to the value $f_1 = 1.027$ Hz.

The finite element method was applied to analyse two plane models BM1 and BM2. The beam element with two nodal points, shown in Fig. 6, was used.

Mechanical properties of an element along its axis was assumed to be constant. The effects of shear deformation and rotary inertia were not taken into account. The structure was divided into 39 finite elements. More information concerning the computations is given in the paper [4]. The results of computation for the models BM1 are listed in Table 1 and 2, respectively.

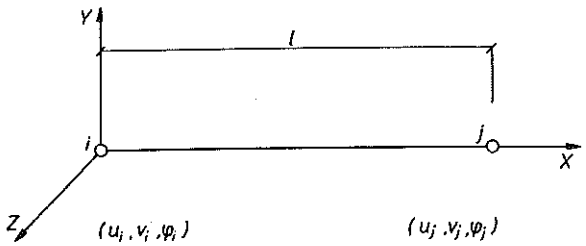


FIG. 6. Beam element for plane computing models.

**Table 1. Natural frequencies. Computing model BM1, (FEM).**

| | BM1 – IC | BM1 – IIA | BM1 – IIB | BM1 – IIC |
|---|---|---|---|---|
| $j$ – | $f_j$ Hz | $f_j$ Hz | $f_j$ Hz | $f_j$ Hz |
| 1 | 0.754 | 0.739 | 0.744 | 0.783 |
| 2 | 1.093 | 1.067 | 1.077 | 1.157 |
| 3 | 1.736 | 1.695 | 1.709 | 1.812 |
| 4 | 1.840 | 1.791 | 1.807 | 1.917 |
| 5 | 2.069 | 2.048 | 2.053 | 2.123 |
| 6 | 2.146 | 2.065 | 2.093 | 2.261 |
| 7 | 2.527 | 2.465 | 2.487 | 2.664 |
| 8 | 2.868 | 2.776 | 2.804 | 3.028 |
| 9 | 3.196 | 3.103 | 3.132 | 3.638 |
| 10 | 3.628 | 3.527 | 3.561 | 3.399 |
| 11 | 3.730 | 3.696 | 3.707 | 3.957 |
| 12 | 4.902 | 4.789 | 4.826 | 5.138 |
| 13 | 5.572 | 5.423 | 5.475 | 5.638 |
| 14 | 5.598 | 5.589 | 5.591 | 5.888 |
| 15 | 7.077 | 6.841 | 6.911 | 7.509 |

As the control method, the Kolousek's slope deflection method was used [5]. The structure was divided into 37 prismatic sections. It was assumed that the sections are perfectly rigid along the longitudinal axis and are deformed only by bending. The effect of shear deformation and rotary inertia were not taken into consideration as previously. The results of computation for both the BM1 and BM2 models are listed in Table 3.

The space computing models (cf. Fig. 5) were analysed with the use of FEM only. The structure was modelled by means of the beam elements. The beam element was assumed to be one-dimensional Cosserat's continuum in which each of its points (cross-section) had six degrees of freedom [6]. The end nodal points of the element $i$, $j$ have, as nodal parameters,

**Table 2. Natural frequencies. Computing model BM2, (FEM).**

| | BM2 – IC | BM2 – IIA | BM2 – IIB | BM2 – IIC |
|---|---|---|---|---|
| $j$ – | $f_j$ Hz | $f_j$ Hz | $f_j$ Hz | $f_j$ Hz |
| 1 | 0.832 | 0.816 | 0.821 | 0.865 |
| 2 | 1.093 | 1.067 | 1.077 | 1.157 |
| 3 | 1.814 | 1.728 | 1.747 | 1.919 |
| 4 | 1.933 | 1.923 | 1.942 | 2.042 |
| 5 | 2.172 | 2.080 | 2.103 | 2.300 |
| 6 | 2.543 | 2.468 | 2.493 | 2.686 |
| 7 | 2.892 | 2.803 | 2.832 | 3.058 |
| 8 | 3.191 | 3.104 | 3.134 | 3.378 |
| 9 | 3.709 | 3.583 | 3.623 | 3.925 |
| 10 | 4.833 | 4.711 | 4.752 | 5.098 |
| 11 | 5.553 | 5.411 | 5.460 | 5.874 |
| 12 | 7.010 | 6.800 | 6.872 | 7.340 |
| 13 | 7.209 | 7.128 | 7.044 | 7.457 |
| 14 | 7.870 | 7.569 | 7.812 | 8.323 |
| 15 | 8.041 | 7.781 | 7.878 | 8.516 |

**Table 3. Natural frequencies. Computing models BM1 and BM2, (KSDM).**

| | BM1 – IIA | BM1 – IIB | BM2 – IIA | BM2 – IIB |
|---|---|---|---|---|
| $j$ – | $f_j$ Hz | $f_j$ Hz | $f_j$ Hz | $f_j$ Hz |
| 1 | 0.739 | 0.744 | 0.922 | 0.822 |
| 2 | 1.066 | 1.076 | 1.067 | 1.077 |
| 3 | 1.707 | 1.726 | 1.727 | 1.747 |
| 4 | 1.839 | 1.857 | 1.972 | 1.991 |
| 5 | 2.071 | 2.093 | 2.071 | 2.093 |
| 6 | 2.367 | 2.390 | 2.507 | 2.532 |
| 7 | 2.707 | 2.735 | 2.818 | 2.845 |
| 8 | 3.067 | 3.097 | 3.070 | 3.100 |
| 9 | 3.467 | 3.502 | 3.508 | 3.547 |
| 10 | 3.726 | 3.746 | 4.883 | 4.926 |
| 11 | 5.098 | 5.137 | 5.384 | 5.435 |
| 12 | 5.390 | 5.441 | 6.757 | 6.833 |
| 13 | 6.761 | 6.838 | 7.264 | 7.340 |
| 14 | 7.287 | 7.363 | 7.422 | 7.501 |
| 15 | 7.424 | 7.503 | 8.326 | 8.413 |

the components of the displacement vector $\{\mathbf{u}\}$ and the components of the rotation vector $\{\phi\}$. The middle nodal point $k$ has, as nodal parameters, the components of the displacement vector $\{\mathbf{u}\}$ only (Fig. 7).

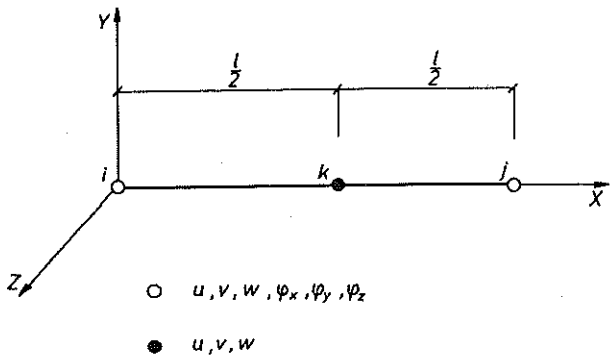


FIG. 7. Beam element for space computing models.

The Mindlin's bending theory was used. Mechanical properties along the axis of an element assumed to be constant. The structure was divided into 90 finite elements where 181 nodal points arose. The results of computation for both space models BM1S and BM2S are listed in Table 4. The mode shapes of vibration are shown in Fig. 8.

**Table 4. Natural frequencies. Computing models BM1S and BM2S, (FEM).**

| | BM1S – IIC | BM2S – IIC |
|---|---|---|
| $j$ – | $f_j$ Hz | $f_j$ Hz |
| 1 | 0.786 | 0.865 |
| 2 | 1.185 | 1.185 |
| 3 | 1.204 | 1.204 |
| 4 | 1.658 | 1.658 |
| 5 | 1.744 | 1.873 |
| 6 | 1.884 | 2.068 |
| 7 | 2.079 | 2.268 |
| 8 | 2.268 | 2.689 |
| 9 | 2.659 | 3.053 |
| 10 | 3.012 | 3.369 |
| 11 | 3.369 | 3.400 |

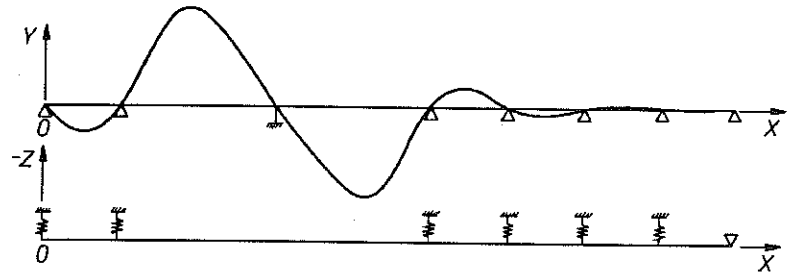


$f_1 = 0.865$ Hz

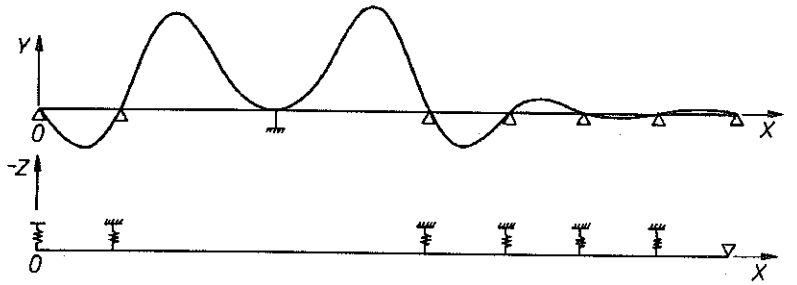


$f_2 = 1.185$ Hz

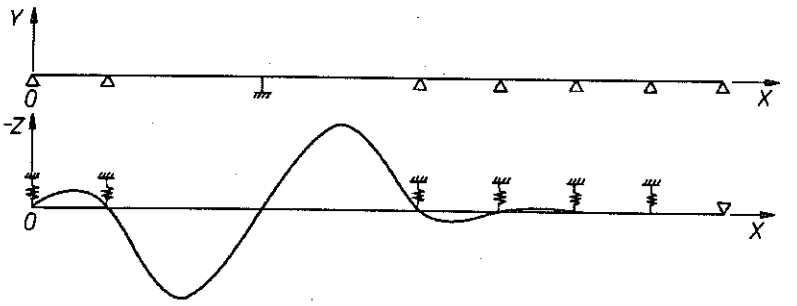


$f_3 = 1.204$ Hz

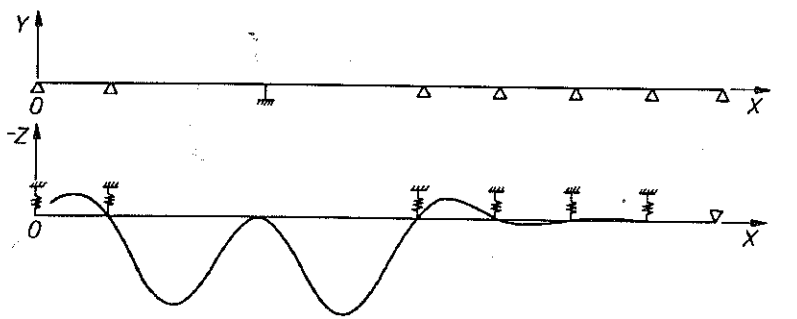


$f_4 = 1.658$ Hz

[FIG. 8]

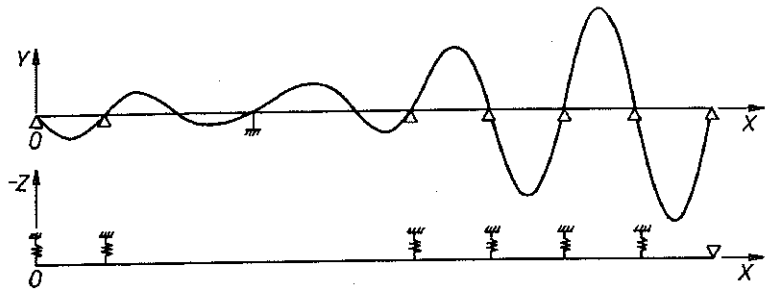


$f_5 = 1.873$ Hz

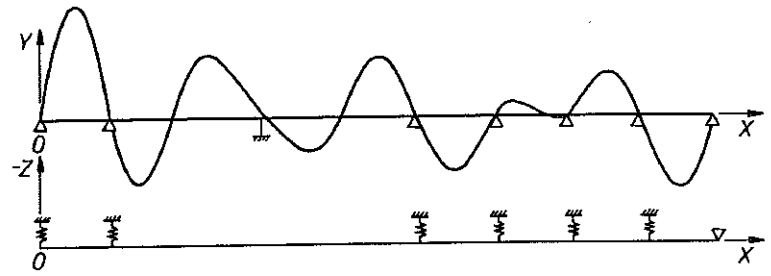


$f_6 = 2.068$ Hz

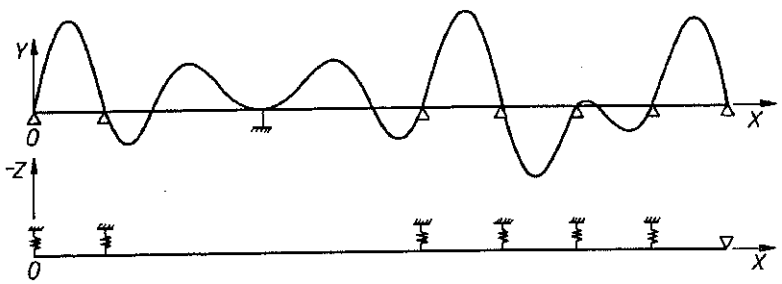


$f_7 = 2.268$ Hz

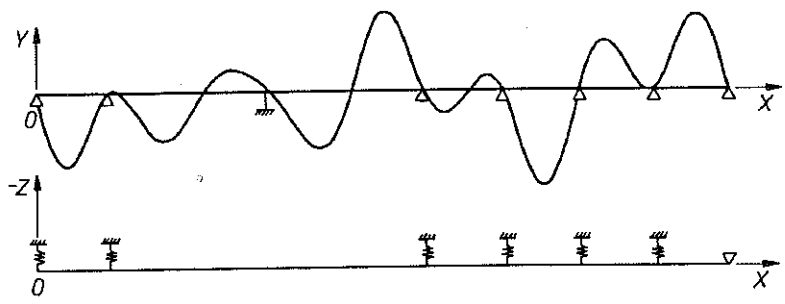


$f_8 = 2.689$ Hz

[FIG. 8]

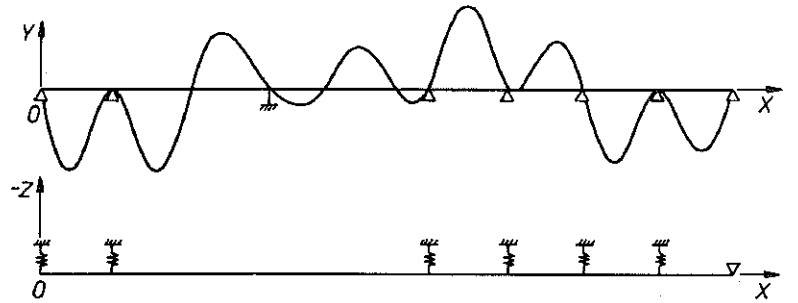


$f_9 = 3.053$ Hz

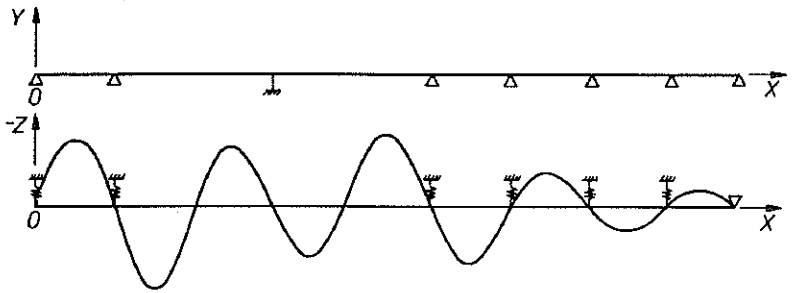


$f_{10} = 3.369$ Hz

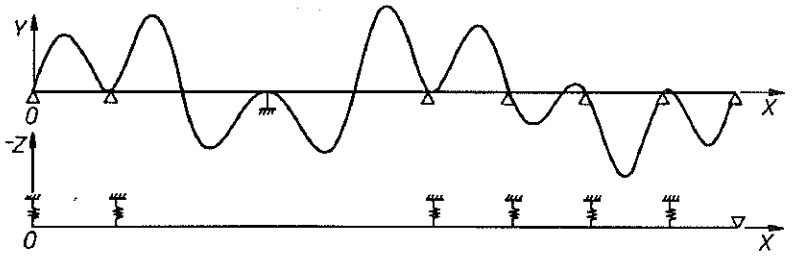


$f_{11} = 3.400$ Hz

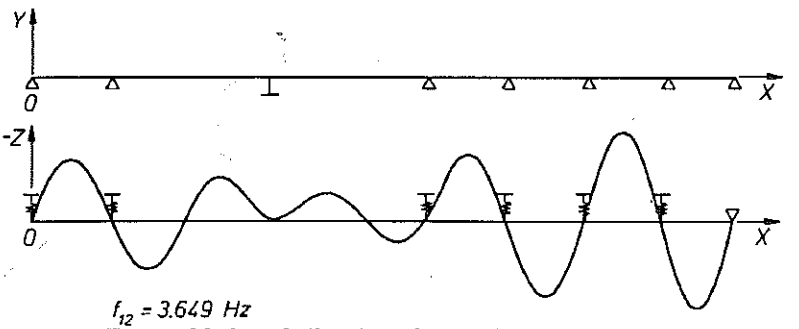


$f_{12} = 3.649$ Hz

FIG. 8. Modes of vibration. Computing model BM2S.

## 4. Dynamic coefficient

### *4.1. Method of solution*

The dynamic coefficient $\delta$, presented in this paper, was determined from the bridge response induced by simultaneous runs of two vehicles arranged in one row, when they crossed the bridge.

The equations of motion describing the synchronous vibration of the system "vehicle-bridge" were derived in the form of the second-order differential Lagrange's equations

$$\frac{d}{dt}\frac{\partial T(t)}{\partial\left(\frac{dq}{dt}\right)} - \frac{\partial T(t)}{\partial q} + \frac{\partial V(t)}{\partial q} + \frac{\partial D(t)}{\partial\left(\frac{dq}{dt}\right)} = 0. \tag{4.1}$$

Functions $a(t)$, $z(t)$, $\varphi(t)$ have been consecutively substituted for the generalized coordinate $q$.

$V(t)$ is the potential energy of the system,

$T(t)$ is the kinetic energy of the system,

$D(t)$ is the energy absorbed by vehicle absorber and bridge in a time unit,

$\varphi(t)$ is the rotation angle about the centroid of the suspended vehicle mass in vertical plane,

$z(t)$ is the vertical amplitude of vibration of the suspended vehicle mass centroid,

$a(t)$ is the coefficient of proportionality.

The following simplifying assumptions are accepted:

- vehicle is considered as a plane model (Fig. 9),

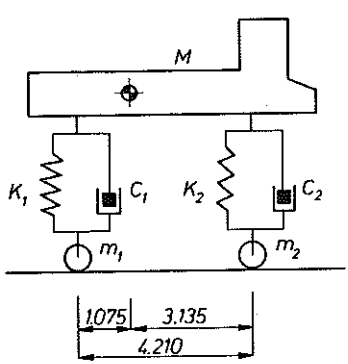


$m_1 = 2140$ kg
$m_2 = 910$ kg
$M = 23650$ kg
$C_1 = 130100$ Ns/m
$C_2 = 22847$ Ns/m
$K_1 = 1322127$ MN/m
$K_2 = 0258322$ MN/m

Fig. 9. Vehicle model.

• the model is considered as Bernouli – Euler's beam model with only linear deformations,

• vehicle suspension elements are linearly elastic,

• vehicle absorbers have viscous damping,

• damping is proportional to the vehicle vibration velocity,

• elastic and damping vehicle tire properties are neglected,

• vehicle moves with constant speed,

• dynamic bending line of beam axis is proportional to the bending line caused by the static load (Fig. 10),

• vehicle remains in contact with the bridge during the whole time of travelling,

• if the contact force is less than zero, in the next step the stiffness of suspension elements of the model will be taken as zero,

• pavement irregularities are simulated by random discrete values in the range $\langle -7;\ +7\rangle$ mm.

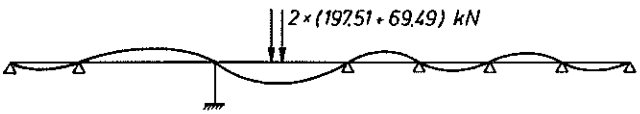


FIG. 10. Assumed bridge deformation.

The system of equations has been solved using the Merson's modification of classical numerical integration method of Runge – Kutta.

The calculation of the dynamic midspan deflection was performed with the values of vehicle parameters (mass, suspension characteristics, speed) corresponding to the values used during the bridge test.

### *4.2. Results of computation*

The runs of vehicles through a norm plank placed at midspan of each span and runs of vehicles without a norm plank, were numerically simulated. The dynamic coefficients $\delta$ and $\delta^*$ as functions of vehicle speed were calculated for each span. In this paper, the results of computation for the 2nd and 3rd spans at those speeds of vehicle motion which were realized during the dynamic loading test are presented (see Table 5 and Table 6).

**Table 5. Calculated dynamic coefficients in the 2nd span. Runs of vehicles through a norm plank placed at midspan.**

| $j$ – | speed km/h | direction – | $\delta$ – | $\delta^*$ – |
|---|---|---|---|---|
| 1 | 10.30 | $B-V$ | 1.133 | 1.0121 |
| 2 | 20.05 | $B-V$ | 1.109 | 1.0099 |
| 3 | 29.48 | $B-V$ | 1.112 | 1.0101 |
| 4 | 40.20 | $B-V$ | 1.192 | 1.0174 |
| 5 | 47.27 | $B-V$ | 1.248 | 1.0225 |
| 6 | 49.53 | $B-V$ | 1.262 | 1.0238 |
| 7 | 55.28 | $B-V$ | 1.315 | 1.0286 |
| 8 | 10.32 | $V-B$ | 1.134 | 1.0121 |
| 9 | 19.97 | $V-B$ | 1.110 | 1.0100 |
| 10 | 30.96 | $V-B$ | 1.121 | 1.0110 |
| 11 | 39.94 | $V-B$ | 1.191 | 1.0173 |
| 12 | 49.93 | $V-B$ | 1.266 | 1.0242 |
| 13 | 57.33 | $V-B$ | 1.322 | 1.0293 |
| 14 | 58.97 | $V-B$ | 1.329 | 1.0299 |

**Table 6. Calculated dynamic coefficients in the 3rd span. Smooth runs of vehicles.**

| $j$ – | speed km/h | direction – | $\delta$ – | $\delta^*$ – |
|---|---|---|---|---|
| 1 | 5.10 | $B-V$ | 1.019 | 1.0017 |
| 2 | 10.20 | $B-V$ | 1.032 | 1.0028 |
| 3 | 19.82 | $B-V$ | 1.026 | 1.0023 |
| 4 | 30.58 | $B-V$ | 1.027 | 1.0024 |
| 5 | 40.03 | $B-V$ | 1.028 | 1.0024 |
| 6 | 49.38 | $B-V$ | 1.027 | 1.0024 |
| 7 | 54.31 | $B-V$ | 1.032 | 1.0028 |
| 8 | 64.50 | $B-V$ | 1.027 | 1.0024 |
| 9 | 5.05 | $V-B$ | 1.036 | 1.0032 |
| 10 | 10.10 | $V-B$ | 1.037 | 1.0033 |
| 11 | 20.14 | $V-B$ | 1.024 | 1.0021 |
| 12 | 30.33 | $V-B$ | 1.019 | 1.0017 |
| 13 | 33.30 | $V-B$ | 1.032 | 1.0028 |
| 14 | 49.88 | $V-B$ | 1.017 | 1.0015 |
| 15 | 51.78 | $V-B$ | 1.027 | 1.0024 |
| 16 | 58.75 | $V-B$ | 1.039 | 1.0035 |

## 5. Experimental verification

The dynamic loading test was performed in September 1990 under management of prof. Bencat from UnTC in Žilina [7].

The bridge structure was excited:

a) by smooth runs of 2 vehicles T815 in both directions,

b) by runs of 2 vehicles T815 in both directions through a norm plank,

c) by runs of 2 vehicles T815 with critical speed by sudden breaking in the 2nd and 3rd spans,

d) by blasting of impulse rocket engines.

For comparison, some results of the experimental investigations are presented.

The measured dynamic coefficients $\delta$ and $\delta^*$ for the center of the 2nd span at runs of 2 vehicles T815 through a norm plank placed in the middle of the span, and the ones for the middle of the 3rd span at smooth runs of 2 vehicles T815, are given in this paper. The comparison of calculated and measured dynamic coefficients is seen in Figs. 11 to 14.

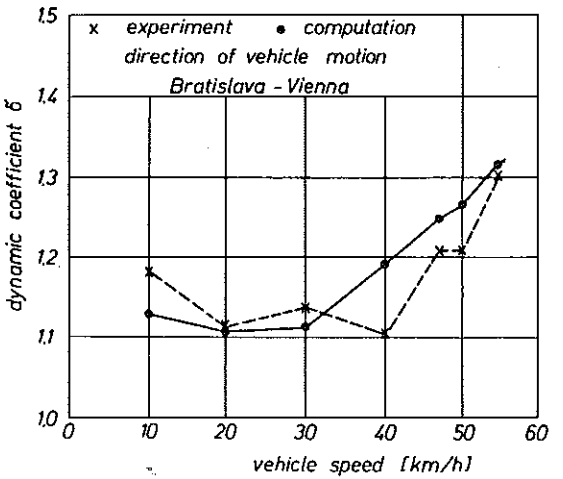


Fig. 11. Calculated and measured dynamic coefficients in the 2nd span. Runs over a norm plank placed at midspan. Direction of vehicle runs: Bratislava – Vienna.

The first 8 natural frequencies of the bridge obtained on the basis of the frequency analysis of records of the vibration are given in Table 7, where the calculated natural frequencies for the computing models BM2-IIC and BM2S-IIC are also listed. The results obtained by means of these computing models correspond relatively well to the experimentally determined frequencies.

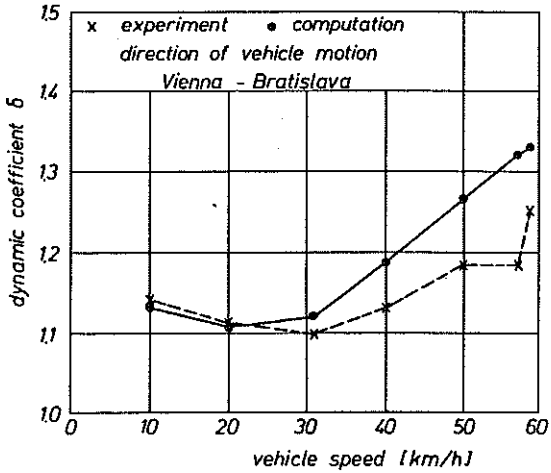


FIG. 12. Calculated and measured dynamic coefficients in the 2nd span. Runs over a norm plank placed at midspan. Direction of vehicle runs: Vienna – Bratislava.

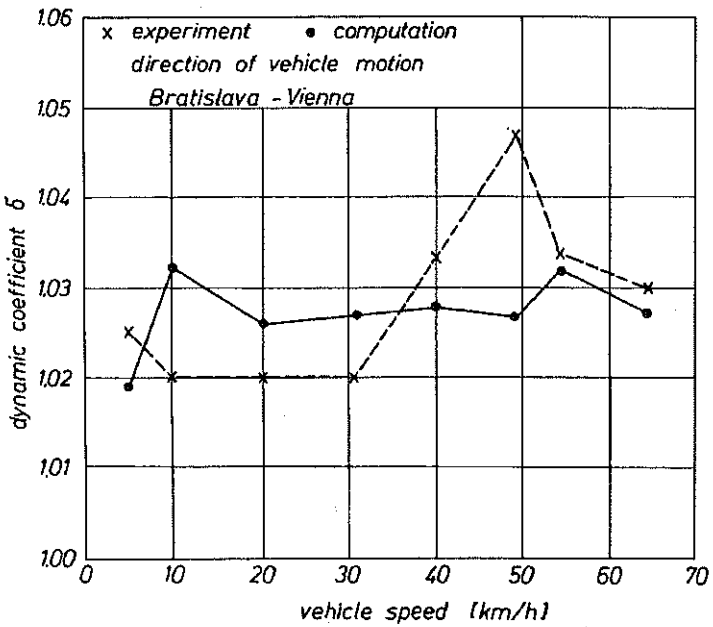


FIG. 13. Calculated and measured dynamic coefficients in the 3nd span. Smooth runs. Direction of vehicle runs: Bratislava – Vienna.

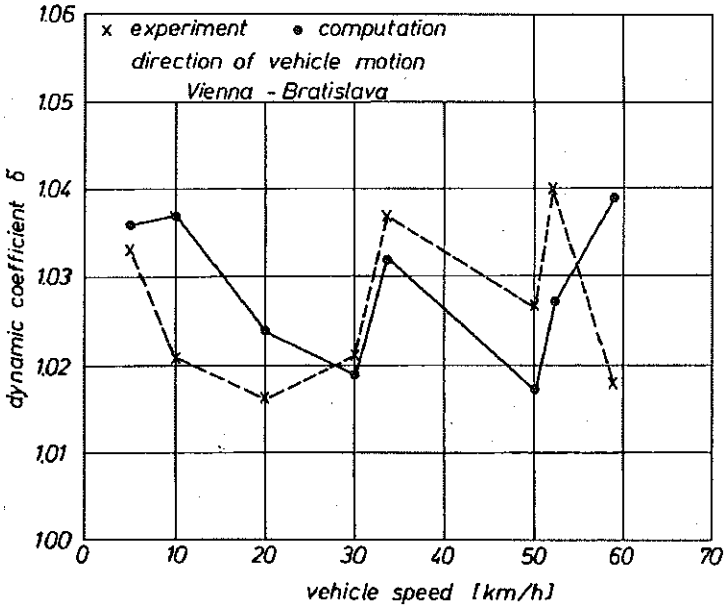


FIG. 14. Calculated and measured dynamic coefficients in the 3nd span. Smooth runs. Direction of vehicle runs: Vienna – Bratislava.

**Table 7. Calculated and observed natural frequencies.**

| | BM2 – IIC | | BM2S – IIC | experiment |
|---|---|---|---|---|
| $j$ – | $f_j$ $Hz$ | $j$ – | $f_j$ $Hz$ | $f$ $Hz$ |
| 1 | 0.865 | 1 | 0.865 | 0.875 |
| 2 | 1.157 | 2 | 1.185 | 1.187 |
| – | – | 3 | 1.204 | 1.218 |
| – | – | 4 | 1.658 | 1.562 |
| 3 | 1.919 | 5 | 1.873 | 1.900 |
| 4 | 2.042 | 6 | 2.068 | 2.148 |
| 5 | 2.301 | 7 | 2.268 | 2.275 |
| 6 | 2.686 | 8 | 2.689 | 2.775 |

The first 2 modes of natural vibration were most effectively excited by means of the impulse rocket engines (IRE) what is proved by the power spectral densities (PSD) of deviations, given in Figs. 15 and 16.

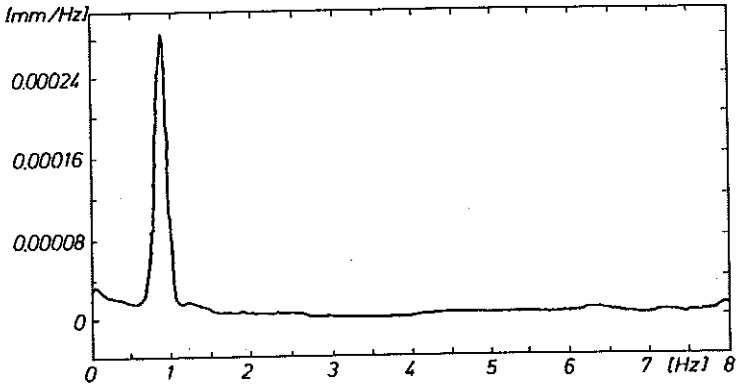


FIG. 15. PSD of deviations in the middle of the 3rd span. Synchronously blasted IRE in the 2nd, 4th and the 6th spans.

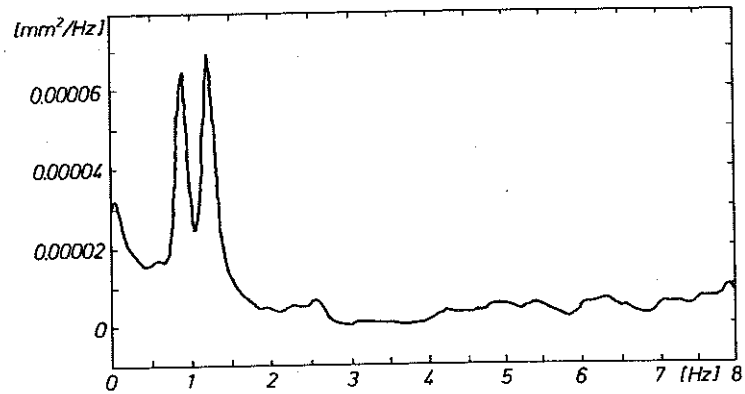


FIG. 16. PSD of deviations in the middle of the 3rd span. Synchronously blasted IRE in the 2nd and 3rd spans.

## 6. CONCLUSIONS

The dynamic calculation was done on the basis of the valid working drawing plans, and on the basis of design consultations, submitted 9 months before doing the dynamic loading test. The dynamic loading test verified that the bridge fulfils all the design parameters. A very good agreement between the calculated and measured natural frequencies was found in the test. The frequency analysis was done for 608 records of the vibration (18 measured points $\times 38$ vibration records).

All the experimentally found values of the dynamic coefficients for every bridge span fulfilled the basic criterion (1.4) required by the Standard CSN 73 6209 [1]. The used calculation of the dynamic coefficient with respect to the accepted simplifying assumptions can be regarded only as approximate.

On the other hand, acceptable results were obtained. For the solution of this task, a computer program was applied with the possibility of graphic output of the results and succesive statistic analysis.

## REFERENCES

1. *CSN 73 6209 Loading Tests of Bridges* [in Czech], Institute for Standardization and Measurements, Prague 1987.
2. J. MELCER *et. al., Dynamic computation of the Youth Bridge D 201 HMO across the Danube in Bratislava – the right-hand bridge* [in Slovak], University of Transport and Communications, Žilina 1989.
3. *CSN 73 6203 Load of bridges* [in Czech], Institute for Standardization and Measurements, Prague 1987.
4. C.T.F. ROSS, *Finite element methods in structural mechanics*, Ellis Horwood Limited, England 1985.
5. V. KOLOUSEK, *Dynamics of building structures 2* [in Czech], SNTL, Prague, the 3rd edition, 1980.
6. V. KOLAR, *Computing model of classical bar and Mindlin's bar in the present construction practice* [in Czech], Designing and Traffic Engineering Institute Dopravoprojekt, Brno 1982.
7. J. BENCAT *et. al., Report on dynamic loading test results of the highway bridge D 201 HMO over the Danube in Bratislava* [in Slovak], University of Transport and Communications, Žilina 1990.

**UNIVERSITY OF TRANSPORT AND COMMUNICATIONS,**
**ŽILINA, THE SLOVAK REPUBLIC.**

*Received October 12, 1994.*